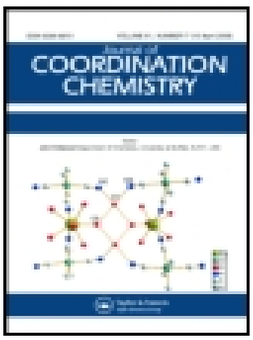

Journal of Coordination Chemistry

ISSN: 0095-8972 (Print) 1029-0389 (Online) Journal homepage: http://www.tandfonline.com/loi/gcoo20

1-(3-Chlorophenyl)-4-(3-phenylseleno propyl) piperazine (L); Synthesis, spectroscopic characterization, DFT studies, antimicrobial evaluation and its reactivity towards group 12 metal chlorides

Muzzaffar A. Bhat, Shabir H. Lone & Sanjay K. Srivastava

To cite this article: Muzzaffar A. Bhat, Shabir H. Lone & Sanjay K. Srivastava (2018): 1-(3-Chlorophenyl)-4-(3-phenylseleno propyl) piperazine (L); Synthesis, spectroscopic characterization, DFT studies, antimicrobial evaluation and its reactivity towards group 12 metal chlorides, Journal of Coordination Chemistry

To link to this article: https://doi.org/10.1080/00958972.2018.1489126

Publisher: Taylor & Francis
Journal: *Journal of Coordination Chemistry*
DOI: http://doi.org/10.1080/00958972.2018.1489126

1-(3-Chlorophenyl)-4-(3-phenylseleno propyl) piperazine (L); Synthesis, spectroscopic characterization, DFT studies, antimicrobial evaluation and its reactivity towards group 12 metal chlorides

MUZZAFFAR A. BHAT*†‡, SHABIR H. LONE§ and SANJAY K. SRIVASTAVA*†

†School of Studies in Chemistry, Jiwaji University, Gwalior 474011, India
‡Department of Chemistry, Islamic University of Science and Technology, Awantipora, Kashmir, 192122, India
§Department of Chemistry, Govt Degree College Anantnag, Kashmir 192101, India

$C_6H_5Se^-Na^+$ (generated *in situ* by $NaBH_4$ reduction of $(C_6H_5Se)_2$) on reaction with $ClC_3H_6C_4H_8N_2ClC_6H_5$ under N_2 atmosphere results in $C_6H_5SeC_3H_6C_4H_8N_2ClC_6H_5$ (L) as a cream-colored solid. Its 1:1 metal complexes having the general formula $[MLX_2]$, where M = Zn, Cd, Hg and X = Cl, have been prepared. Ligand L and its complexes **1-3** are characterized on the basis of physico-chemical and spectral (FT-IR, ESI Mass, ^1H, ^{13}C, DEPT 135° ^{13}C $\{^1H\}$ and $^{77}Se\{^1H\}$ NMR) studies. IR spectroscopy revealed that L is coordinated solely through selenium and nitrogen to zinc, cadmium and mercury ions forming a six-membered chelate ring around M(II) ions. Elemental analysis measurements along with ^1H, ^{13}C, DEPT 135° ^{13}C $\{^1H\}$ and ESI mass data also confirm the bidentate coordination mode of the ligand. Moreover, the coordination from selenium atom is also supported by the downfield shift of signal in $^{77}Se\{^1H\}$ NMR spectroscopy. Using DFT-based optimization of structures, the HOMO-LUMO energy gaps and molecular electrostatic potential (MEP) surface of ligand L and complexes **1-3** were theoretically calculated at the B3LYP/LANL2DZ level of theory. Ligand L and complexes **1-3** display significant antibacterial and antifungal activity.

Keywords: Reduction; Selenium; Bidentate; Coordination; DFT; Biological activity

*Corresponding authors. Email: muzzaffarbhat9@gmail.com, muzzaffarbhat9@yahoo.com (M.A. Bhat); sksrivas7@yahoo.com (S.K. Srivastava)

1. Introduction

Group 12 metals (Zn, Cd, Hg) are considered to be the most covalent and chalcophilic in the periodic table. The chemistry of group 12 metal chalcogenides has been extensively studied due to their applications in the field of nanomaterials [1] and opto-electronics [2]. Due to their importance, the preparation and structural characterization of group 12-16 complexes as single-source stoichiometric precursors have continued to draw the attention of chemists. Various research groups have reported that $[M(ER)_2]$ complexes (M = Zn, Cd or Hg; E = S, Se or Te; R = aryl) can be utilized as such precursors [3]. However, these compounds are generally polymeric in the solid state, very difficult to isolate in the crystalline form, relatively insoluble in hydrocarbon solvents and therefore, very difficult to be purified and characterized [4]. Organoselenium chemistry has been exploited to present an extensive range and high diversity of products that find an inevitable place in the area of synthetic applications [5, 6]. In addition, organoselenium compounds are known to be suitable antioxidants because of their unique ability to imitate the enzymatic activities of glutathione peroxidase (Gpx) that catalyzes the decomposition of hydroperoxides in various biochemical reactions [7, 8]. Organoselenium compounds containing selenium in bivalent oxidation state play a prominent role in coordination chemistry [9, 10]. An extensive use of organoselenium compounds in semiconductors and Metal Organic Chemical Vapor Deposition (MOCVD) techniques consign these compounds a noticeable position in electronic chemistry [11, 12]. A number of methods [13-17] have been developed to obtain an array of aryl/alkyl monoselenides and symmetrical diselenides [18-20]. Symmetrical dialkyl/diaryl monoselenides have also been prepared by the cleavage of dialkyl/diaryl diselenides [21-23], while other methods use transition metal complexes [24-26]. Synthesis, ligation behavior and applications of N-{2-(4-methoxyphenyltelluro)ethyl}morpholine with palladium(II), half-sandwich ruthenium(II) complexes of N-{2-(arylchalcogeno)ethyl}morpholine as useful catalysts for oxidation of alcohols and rhodium(III) complexes of N-{2-(arylseleno/telluro)ethyl}morpholine as catalysts suitable for transfer hydrogenation of ketones has been reported by Singh and co-workers. Recently, the same group carried out the synthesis and structural chemistry of N-{2-(arylthio/seleno)ethyl}morpholine/piperidine-palladium(II) complexes as potent catalysts for the Heck reaction [27].

Our continuing interest in the chalcogen-based ligands [28-33] prompted us to report the novel synthesis and coordination behavior of seleno-piperazine ligand containing nitrogen donors in conjunction with selenium and thus the ligation behavior of (Se, N, N) type hybrid donor ligands with group 12 metal halides.

2. Experimental

2.1. *Materials and methods*

1-(3-Chlorophenyl)-4-(3-chloropropyl)piperazine hydrochloride was procured from Sigma-Aldrich (USA) and used as received. Solvents were dried and distilled before use by well-known standard procedures [34]. The molar conductance of the compounds were measured at r.t. (30±2 °C) using a dip-type conductivity cell (cell constant = 0.95) on an ELICO conductivity meter model 127 in anhydrous dimethylsulfoxide (DMSO). The FT-IR spectra of the compounds were recorded on a Nicolet Protége 460 FT-IR spectrometer (KBr, 4000-340 cm^{-1}). ^{1}H, ^{13}C $\{^{1}H\}$, DEPT 135° ^{13}C $\{^{1}H\}$ and ^{77}Se {1H} NMR spectra were recorded on a Bruker Spectrospin DPX-300 NMR spectrometer at 300.13, 50.47, 50.47 and 57.24 MHz, respectively. ESI-mass spectra were recorded on a WATERS-Q-TOF premier-HAB213 spectrometer. The samples (dissolved in methanol and acetonitrile) were introduced into the ESI source through a syringe pump at the rate 3 µL/min. The ESI capillary was set at 3.5 kV and the cone voltage was 40 V.

All the computations are carried out using GAUSSIAN 09 software [35]. The DFT modeling method, using the hybrid B3LYP [36] functional was used to calculate L and complexes **1-3** with the basis set combination 6-311 G(d,p) [37]. The antimicrobial activity was performed against one bacterial and one fungal strain. The organisms selected were the Gram-positive *Staphylococcus aureus* (NCIM2063, Sa) and the fungal strain *Aspergillus niger* (ATCC-6275, An). The method employed to determine the MIC values was serial tube dilution method [38] for ligand as well as complexes. 2.00 mg of each tested compound was placed in vials separately and 2 mL of DMSO was added and a solution of the concentration 1.00 mg/mL was obtained. *Staphyllococus aureus* was grown at 37 °C in nutrient agar medium and then diluted in sterile nutrient broth medium to get a suspension containing about 10^7 cells/mL and finally used as the inoculum. As much as 11 test tubes were taken, 9 of which were marked as T_1, T_2, T_3, T_4, T_5, T_6, T_7, T_8 and T_9 and the remaining two were assigned as T_M (medium) and T_{MI} (medium+inoculum). 1 mL of nutrient broth medium was poured into all 11 test tubes. The tubes

were plugged with cotton and sterilized in an autoclave. The tubes were then cooled and 1 mL of the sample solution was added in the first test tube and mixed well followed by transference of 1 mL of the contents to the second test tube; this process of serial dilution was done up to the ninth test tube. 10 μL of properly diluted inoculum was added to each of the nine test tubes and mixed well. 10 μL of the inoculum was added to the test tube T_{MI} to observe the growth of the organism in the medium used. To confirm the sterility of the medium the controlled test tube T_M containing only the medium was used. All the test tubes were incubated at 37 °C. The same experiment was done with medium, DMSO, and inoculum without compound to ensure that the DMSO has no inhibitory effect. The test tube number in which the first sign of growth of the organism was observed was noted. The MIC was taken as that concentration used in the test tube number just prior to the test tube number where the first sign of growth was observed. This was done for all the compounds and ligand to calculate their MIC values. The same procedure was done to assess the antifungal activity of the compounds except that Potato-Dextrose-Agar medium was used.

2.2. ***Synthesis of 1-(3-chlorophenyl)-4-(3-phenylseleno propyl)piperazine (L)***

To a stirred solution of diphenyl-diselenide (1.57 g, 5 mmol) and sodium hydroxide (0.040 g, 5 mmol) in aqueous THF (20 mL + 0.2 mL H_2O) under dry nitrogen, $NaBH_4$ (0.419 g, 11 mmol) was added in pinches. The orange-yellow color of the diselenide disappeared within few minutes. The resulting colorless sodium phenyl-selenoate solution was allowed to warm to room temperature over 0.25 h. To the clear solution thus formed, 1-(3-chlorophenyl)-4-(3-chloropropyl) piperazine hydrochloride (3.09 g, 10 mmol) was added in pinches. The reaction mixture was stirred overnight at room temperature and then treated with 50 mL of 1 M NaOH solution. Ligand L was extracted into chloroform from this basic solution. The extract was washed with water, dried over anhydrous magnesium sulfate and concentrated under reduced pressure to give a cream-colored viscous oil. It was repeatedly washed with hexane to remove the unreacted diphenyl-diselenide. Solid cream product was precipitated by addition of 2-3 drops of methanol to the viscous mass. It was filtered and dried in *vacuo* (scheme 1).

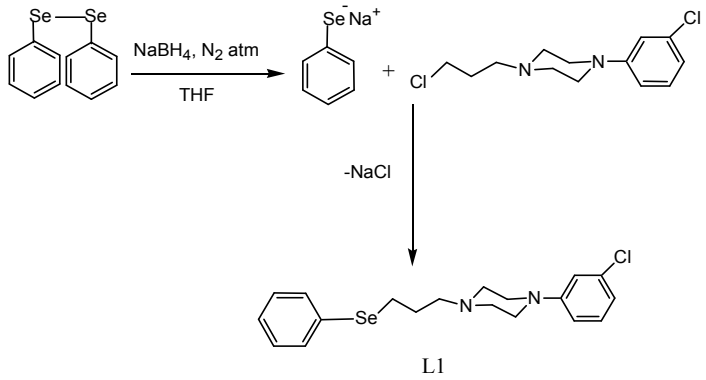

Scheme 1. Synthetic scheme and chemical structure of L.

2.3. *Reaction of L with group 12 metal chlorides*

In a representative experiment, to a solution of L (0.357 g, 1 mmol) in absolute ethanol and anhydrous $ZnCl_2$ (0.360 g, 1 mmol) in the same solvent, were stirred together at r.t. under dry dinitrogen for about 4 h. The precipitated product was filtered and washed several times with petroleum ether (60-80 °C). The product was dried under *vacuo*. Similar complexes were prepared using anhydrous $CdCl_2$ and $HgCl_2$ (99.9% purity) as metal acceptors (scheme 2).

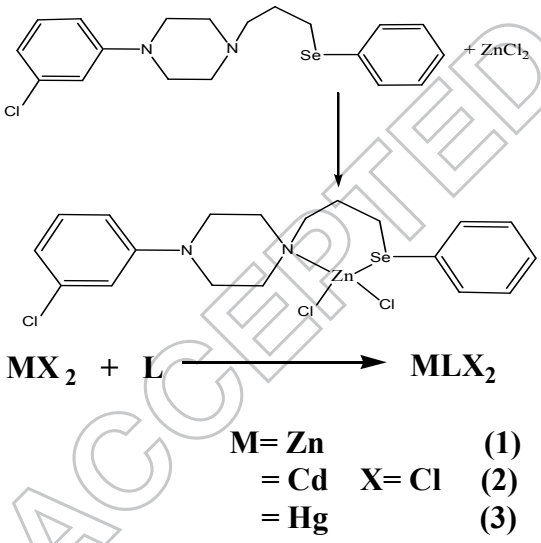

Scheme 2. Synthesis of group 12 metal complexes.

3. Results and discussion

3.1. *General*

The analytical and physical data of L and **1-3** are in agreement with the 1:1 stoichiometry (table 1). L is isolated as solid white product, stable at r.t. and not affected by atmospheric oxygen and moisture. Complexes **1-3** are of 1:1 (donor:acceptor) stoichiometry and are solids, soluble in common organic solvents.

3.2. *Conductance*

The molar conductance (Λ_M) of L and **1-3** has been determined in DMSO 1 mM and the values are given in table 1. Molar conductance of L and **1-3** have been found to be much lower than the value expected for any electrolyte and hence these may be considered to behave as non-electrolyte or non-ionic.

3.3. *ESI Mass spectra*

The ESI mass spectrum of L and complex **3** were recorded using methanol and acetonitrile as solvents and important fragmentation patterns are given in table S1.

In the positive ESI mass spectrum of L, molecular ion peak at 395 with 50% of relative abundance is in agreement with the proposed weight of the compound. Isotopic distribution pattern of chlorine is also observed. The other peaks observed at m/z 240 and m/z 162 are due to [L-(**C_6H_5-Se**)] and [L-(C_6H_5Se)-(**C_3H_7**)], respectively. Another fragment at m/z 85, due to [L-(C_6H_5Se)-(C_3H_7)-(**C_6H_5Cl**)] with 90% of relative abundance, corresponds to the base peak. These signals also exhibit the expected characteristic isotopic distribution pattern of chlorine (figure S1).

In the ESI mass spectrum of **3**, molecular ion peak is observed at m/z 670 with 20% relative abundance, which is in agreement with the proposed molecular weight of the complex. Another peak, observed at m/z 628 with 18% relative abundance, is due to [M-**Cl**] and at m/z 395 is due to the [(M-Cl-(**HgCl**)] as base peak with 100% relative abundance. Other fragments at m/z 226 and m/z 197 are observed due to [(M-Cl-(HgCl)-**$C_6H_5SeCH_2$**] and [(M-Cl-(HgCl)-$C_6H_5SeCH_2$-(**C_2H_5**))] (figure S2).

3.4. *IR Spectra*

Infrared (IR) spectra of L and complexes **1-3** have been recorded using KBr discs (table S2). In the IR spectra of L, the bands due to ν(C-N) group appear at 1178 and 1106 cm^{-1}. The band due to $\nu(C\text{-}H)_{aromatic}$ appears at 3082 cm^{-1}, which shows the presence of phenyl group whereas $\nu(C\text{-}H)_{aliphatic}$ appears at 2854 cm^{-1}. The band of the characteristic group ν(C=C) appears at 1618 cm^{-1}. The band of low intensity at 498 cm^{-1} is assigned to ν(Se-C).

In complexes **1-3**, the bands due to ν(Se-C) group were found slightly shifted to lower frequency (481, 485 and 482 cm^{-1} for complexes **1**, **2** and **3**, respectively) and appeared at 483±2 cm^{-1} in comparison to L, which clearly shows that selenium is involved in coordination to metal salts. Signals due to ν(C-N) group also shifted to lower frequency (1162, 1158 and 1155 cm^{-1} for **1**, **2** and **3**, respectively) and appeared around 1159±4 cm^{-1}. The other characteristic bands are $\nu(C\text{-}C)_{aliphatic}$, $\nu(C\text{-}H)_{aromatic}$ and $\nu(C\text{-}H)_{aliphatic}$ appearing at 1620±10, 3042±10 and 2854±5 cm^{-1}, respectively. DFT assisted IR and experimental IR of ligand L (figure S1) and complex **1** also displayed close agreement.

3.5. *^{1}H NMR Spectra*

^{1}H NMR spectra of L and complexes **1-3** have been recorded in $CDCl_3$ and DMSO-d_6 and values are given in table S3**.** In the ^{1}H NMR spectra of L, two triplets appearing at 2.95-2.98 ppm and 2.46-2.50 ppm are assigned to Se-C**H**$_2$ and C**H**$_2$-N, respectively, while the multiplet at 1.88-1.95 ppm is due to -C**H**$_2$-. Piperazine ring protons appear as two triplets at 2.52-2.55 ppm and 3.28-3.46 ppm. Aromatic protons (Ar-H) attached to Se and Cl are as expected and found at 7.13-7.63 ppm as multiplets (figure S4).

In complexes **1-3**, the signals due to C**H**$_2$-N show deshielding by about ~0.2 ppm (2.54-2.60, 2.57-2.68 and 2.47-2.60 ppm for complexes **1**, **2** and **3**, respectively), suggesting participation of nitrogen in coordination to metal. However, the signals due to Se-C**H**$_2$ and aromatic protons show also deshielding (2.89-2.99, 2.97-3.11 and 2.92-3.09 ppm for **1**, **2** and **3**, respectively) by about ~0.2 ppm relative to free ligand, indicating the involvement of Se also in coordination to metal. -C**H**$_2$- and aromatic protons remain almost at similar positions. The signals due to N-CH_2 merge with signals of DMSO-d_6 in all complexes. Thus, L adopts a bidentate coordination mode in complexes **1-3** (figures S5-S7). Theoretical and experimentally calculated ^{1}H NMR data for ligand L (figure S8) is in very close agreement with each other.

3.6. *$^{13}C\ \{^1H\}$ NMR Spectra*

$^{13}C\ \{^1H\}$ NMR spectra of L and complexes **1-3** have been recorded in $CDCl_3$ and DMSO-d_6 and values are given in table S4. In the $^{13}C\{^1H\}$ NMR spectrum of L, the signals at 27.55, 58.13 and 25.83 ppm are assigned to Se-**C**H_2, **C**H_2-N and -**C**H_2-, respectively. Piperazine ring carbons resonate at 53.19 and 48.82 ppm, respectively. Aryl carbons Ar-C (*ortho*, *meta*, *para*- to Se and Se-C_{ipso}) appear at 130.73, 128.94, 126.98 and 132.73 ppm, respectively. Cl-aryl ring carbons resonate at 152.54, 114.01, 130.21, 115.90, 135.15 and 119.40 ppm (figure S9).

In complexes **1-3**, the Se-**C**H_2 signals are found deshielded (50.55, 45.15 and 45.23 ppm for **1**, **2** and **3**, respectively) by 18-24 ppm with respect to free ligand, indicating the involvement of Se in coordination to metal. The signals due to N-**C**H_2 (57.19, 55.41 and 58.60 ppm for **1**, **2** and **3**, respectively) were also found deshielded which confirms the involvement of N also in coordination to metal salts (figures S10-S12).

3.7. *DEPT 135^o $^{13}C\ \{^1H\}$ NMR*

DEPT 135^o $^{13}C\ \{^1H\}$ NMR spectra of L (figure S13) and complex **1** support the data obtained from $^{13}C\{^1H\}$ NMR and further authenticate the formation of L and complexes. CH_2 carbons of piperazine, Se-CH_2, N-CH_2 and CH_2 are antagonistic to CH carbons of two phenyl rings (figure S14).

3.8. *$^{77}Se\ \{^1H\}$ NMR Spectra*

The $^{77}Se\{^1H\}$ NMR spectra of L and complexes **1** and **2** were recorded using $CDCl_3$ and DMSO as solvent and Me_2Se as an internal standard. In the ^{77}Se NMR (proton decoupled) spectra of L (figure S15), a single peak is observed at δ = 289.74 ppm which is deshielded by 42-54 upon complexation. The deshielding of the selenium atom in complexes supports the formation of metal-selenium bond, which authenticates the findings of IR, ^1H and ^{13}C NMR spectra (figure S16).

3.9. *Optimization*

The optimized structures as deduced from DFT using B3LYP/LANL2DZ level of theory are shown in figure 1. For complexes **1-3**, the geometry around M(II) atom is distorted tetrahedral as

revealed by bond angles. Selected bond lengths and angles of ligand L and complexes **1-3** theoretically calculated at the B3LYP/LANL2DZ are presented in tables 2 and 3.

3.10. *Molecular electrostatic potential surface analysis*

Molecular Electrostatic Potential (MEP) is useful for predicting molecular reaction behavior. It is used to assess the molecular reactivity towards charged reactants and depict the hydrogen bond interactions. MPE surfaces reveal essential characteristics like size, shape and variation of electron density while correlating with dipole moment, partial charges, electronegativity, and chemical reactivity sites located in the molecule. Figure 2 shows the MEP surface of ligand L and complexes **1-3** that were calculated using DFT/B3LYP; LANL2DZ basis set. The pictorial representation with rainbow-colored scheme of electrostatic potential for L lies in the range of -2.970 a.u. to +2.970 a.u. and between -5.830 to +5.830 a.u., -5.524 to +5.524 a.u. and -4.913 to +4.913 a.u. for complexes **1-3**, respectively. In the ESP map for all compounds the region surrounding the chlorine, nitrogen and selenium atoms appear to be darkest red that is one with highest electron density.

3.11. *Frontier molecular orbitals*

Frontier molecular orbitals (FMO) (figure 3) determining the electric optical properties, electronic transitions and kinetic stability [39] FMOs of L and complexes **1-3** were calculated using DFT; BL3YP/LANL2DZ level of theory. As seen in figure 3 for L, HOMOs are located on chloro-phenyl and piperazine part whereas LUMOs are located over phenyl-seleno moiety. The HOMO-LUMO energy gap is 0.18191 eV (table 4). Using this HOMO-LUMO energy gap, chemical descriptors like softness, hardness (η), electronegativity, chemical potential (μ), electron-affinity and ionization energy for both the synthesized compounds were carried out. These properties are calculated as follows [40-42]:

$$\textbf{(1)}\quad \eta = \frac{(I - A)}{2} \qquad \textbf{(2)}\quad \mu = \frac{-(I + A)}{2} \qquad \textbf{(3)}\quad \chi = \frac{(I + A)}{2}$$

where I and A represent ionization potential and electron affinity of the compound, which are actually obtained from HOMO and LUMO energies as I = $-E_{HOMO}$ and A = $-E_{LUMO}$ as per Janak

theorem [43] and Perdew *et al.* [44]. A large HOMO-LUMO gap represents a hard molecule while a small gap indicates a soft or more reactive/less stable molecule.

For complexes **1**-**3**, HOMOs are located over chloro-phenyl and half piperazine ring, leaving phenyl-seleno-propyl and respective metal chlorides blank, however LUMO are homogenously spread over phenyl-seleno and respective metal halides in complexes **1** and **2**, but are restricted over mercury chloride and surroundings in complex **3**.

Chemical potential 'μ' that measures the escaping ability of electrons from an equilibrium system decreases in the order as L (-0.11478) > 1 (-0.12949) > 2 (-0.12977) > 3 (-0.13998). Similarly the global electrophilicity index (ω), a global reactivity index that is related to chemical hardness and chemical potential as introduced by Parr *et al*. [41] represents the measure of the stabilization in energy achieved when the system acquires an additional electronic charge from the environment and is given by $\boldsymbol{\omega} = \mu^2/2\eta$. The corresponding values for L and complexes **1**-**3** are 0.07237, 0.10652, 0.10970 and 0.14841 eV, respectively. All these parameters have been calculated for the target compounds using B3LYP/LANL2DZ basis set and are depicted in table 4.

3.12. *Antimicrobial evaluation*

The antimicrobial activities of the ligand as well as complexes were evaluated by serial tube method and their MIC values are summarized in table 5. Chloromphenicol and flucanozole were used as standard drugs for antibacterial and antifungal activity, respectively. It was observed that the ligand shows lowest antibacterial as well as antifungal effect. However, upon complexation with group 12 metal chlorides its antimicrobial action drastically changes. The highest effect was observed in case of complex **1** which exhibited an MIC of 12 μg/mL against *Aspergillus niger* and 32 μg/mL against *Staphylococcus aureus* followed by complex **2** which exhibited an MIC of 16 μg/mL against *Aspergillus niger* and 40 μg/mL against *Staphylococcus aureus*.

4. Conclusion

1-(3-Chlorophenyl)-4-(3-phenylseleno-propyl)piperazine hydrochloride (**L**) has been synthesized by reacting $ArSe^-$ (generated *in situ* by borohydride reduction of diphenyl-diselenide) with 1-(3-chlorophenyl)-4-(3-chloropropyl)piperazine hydrochloride. Formation of L and its complexes is the first example of novel synthesis where 1-(3-chlorophenyl)-4-(3-chloropropyl)piperazine is

used, which results in the formation of Se,N,N-hybrid donor ligands. Its coordination behavior was examined with Zn, Cd and Hg metal chlorides. Various spectral and analytical data reveal that heteroditopic ligand L (Se,N,N) ligates solely Se and N in complexes **1-3** adopting bidentate mode of ligation. Moreover the coordination from selenium atom is also supported by the downfield shift of signal in $^{77}Se\{^{1}H\}$ NMR spectroscopy.

Using DFT-based optimization of structures, the HOMO-LUMO energy gaps and molecular electrostatic potential (MEP) surface of ligand L and complexes **1-3** were theoretically calculated at the B3LYP/LANL2DZ level of theory. These complexes adopt distorted tetrahedral geometry around M(II) ions as revealed by bond angles. Hybrid ligand (L) (Se,N,N) ligates solely through Se and N in complexes **1-3** adopting bidentate mode of coordination. HOMO-LUMO energy gap was calculated which allowed the calculation of relative properties like chemical hardness, chemical inertness, chemical potential, nucleophilicity and electrophillicity index of the synthesized products. The experimentally obtained IR and NMR results showed a good correlation with those of the theoretical ones. Ligand L and complexes **1-3** display significant antibacterial and antifungal activity.

Acknowledgements

The authors are very thankful to IIIM Srinagar and IIT Delhi for ^{1}H, ^{13}C, DEPT 135° ^{13}C, ^{77}Se NMR and elemental analysis. We are also thankful to Department of Chemistry, Dr. H.S. Gour University, Sagar for IR analysis and SIAF IIT Kanpur for mass analysis.

References

[1] (a) M.A. Malik, P. O'Brien, N. Revaprasadu. *Chem. Mater.*, **14**, 2004 (2002). (b) M. Afzaal, M.A. Malik, P. O'Brien. *J. Mater. Chem.*, **20**, 4031 (2010). (c) A.M. Smith, S. Nie. *Acc. Chem. Res.*, **43**, 190 (2010). (d) X. Peng. *Acc. Chem. Res.*, **43**, 1387 (2010). (e) E.S. Shibu, M. Hamada, S. Nakanishi, S. Wakida, V. Biju. *Coord. Chem. Rev.*, **263**, 2 (2014). (f) J.B. Blanco-Canosa, M. Wu, K. Susumu, E. Petryayeva, T.L. Jennings, P.E. Dawson, W.R. Algar, I.L. Medintz. *Coord. Chem. Rev.*, **263**, 101 (2014). (g) S.R. Alvarado, Y. Guo, T. Purnima, A. Ruberu, E. Tavasoli, J. Vela. *Coord. Chem. Rev.*, **263**, 182 (2014).

[2] (a) M.J. Bowers, J.R. McBride, S.J. Rosenthal. *J. Am. Chem. Soc.*, **127**, 15378 (2005). (b) P.O. Anikeeva, J.E. Halpert, M.G. Bawendi, V. Bulovic. *Nano Lett.*, **9**, 2532 (2009). (c) H.V. Demir, S. Nizamoglu, T. Erdem, E. Mutlugun, N. Gaponik, A. Eychmüller. *Nano Today*, **6**, 632 (2011). (d) H. Shen, S. Wang, H. Wang, J. Niu, L. Qian, Y. Yang, A. Titov, J. Hyvonen, Y. Zheng. L. Li. *ACS Appl. Mater. Interfaces*, **5**, 4260 (2013). (e) L.-J. Zhang, X.-C. Shen, H. Liang, F.-Y. Chen, H.-J. Huang. *New J. Chem.*, **38**, 448 (2014).

[3] (a) M.L. Steigerwald, C.R. Sprinkle. *J. Am. Chem. Soc.*, **109**, 7200 (1987). (b) J.D. Brennan, T. Siegrist, P.J. Carroll, S.M. Struczynski, L.E. Brus, M.L. Steigerwald. *J. Am. Chem. Soc.*, **111**, 4141 (1989). (c) P. O'Brien. *Chemtronics*, **5**, 61 (1991). (d) J. Arnold, J.M. Walker, K.M. Yu, P.J. Bonasia, A.L. Seligson, E.D. Bourret. *J. Cryst. Growth*, **124**, 647 (1992). (e) S.S. Garje, J.S. Ritch, D.J. Eisler, M. Afzaal, P. O'Brien, T. Chivers. *J. Mater. Chem.*, **16**, 966 (2006).

[4] (a) I.G. Dance. *Polyhedron*, **5**, 1037 (1986). (b) H.J. Gysling, in The Chemistry of Organic Selenium and Tellurium Compounds, S. Patai, Z. Rapport (Eds.), Wiley, New York, **1 (18)**, 679 (1986). (c) P.J. Blower, J.R. Dilworth. *Coord. Chem. Rev.*, **76**, 121 (1987). (d) B. Krebs, G. Henkel. *Angew. Chem., Int. Ed. Engl.*, **30**, 769 (1991).

[5] T.G. Back, Topics in Current Chemistry, Organoselenium Chemistry - Modern Developments in Organic Synthesis, Springer, Germany (2000).

[6] T.G. Back, Selenium: Organoselenium Chemistry in Encyclopedia of Inorganic Chemistry, John Wiley and Sons, Chichester, England (1994).

[7] T.G. Back, Z. Moussa, M. Pervez. *Angew. Chem. Int. Ed.*, **43**, 1268 (2004).

[8] S. Mao, Z. Dong, J. Liu, X. Li, G. Luo, J. Shen. *J. Am. Chem. Soc.*, **127**, 11588 (2005).

[9] E.G. Hope, W. Levason. *Coord. Chem. Rev.*, **122**, 109 (1993).

[10] C.O. Kienitz, C. Thöne, P.G. Jones. *Inorg. Chem.*, **35**, 3990 (1996).

[11] M. Bochman. *Chem. Vap. Depos.*, **2**, 85 (1996).

[12] M. Beradini, T.J. Emge, J.G. Brennan. *J. Am. Chem. Soc.*, **116**, 6941 (1994).

[13] J. Müller, A. Terfort. *Inorg. Chim. Acta*, **359**, 4821 (2006).

[14] S.J. Dunne, L.A. Summers, E.I. von Nagy Felsobuki. *J. Heterocyl. Chem.*, **32**, 1671 (1995).

[15] W.S. Haller, K.J. Irgolic. *J. Organomet. Chem.*, **38**, 97 (1972).

[16] D.L. Klayman, T.S. Griffin. *J. Am. Chem. Soc.*, **95**, 197 (1973).

[17] L. Syper, J. Mlöchowski. *Synthesis*, 439 (1984).

[18] K. Shimada, S. Oikawa, H. Nakamura, A. Moro-oka, M. Kikuchi, A. Maruyama, T. Suzuki, H. Kogawa, Y. Inoue, Y. Gong, S. Aoyagi, Y. Takikawa. *Bull. Chem. Soc. Jpn.*, **78**, 899 (2005).

[19] K.B. Sharpless, R.F. Lauer. *J. Am. Chem. Soc.*, **95**, 2697 (1973).

[20] J.A. Gladysz, J.L. Hornby, J.E. Garbe. *J. Org. Chem.*, **43**, 1204 (1978).

[21] H. Suzuki, H. Abe, A. Osuka. *Chem. Lett.*, 151 (1981).

[22] A. Osuka, N. Ohmasa, H. Suzuki. *Synth. Commun.*, 857 (1982).

[23] C.M. Andersson, A. Hallberg, M. Linden, R. Brattsand, P. Moldeus, I. Cotgreave. *Free Radical Biol. Med.*, **16**, 7 (1994).

[24] Y. Nishiyama, K. Tokunaga, N. Sonoda. *Org. Lett.*, **1**, 1725 (1999).

[25] H.J. Cristau, B. Chabaud, R. Labaudiniere, H. Cristol. *Organometallics*, **4**, 657 (1985).

[26] K. Ajiki, M. Hirano, K. Tanaka. *Org. Lett.*, **7**, 4193 (2005).

[27] P. Singh, A.K. Singh. *Eur. J. Inorg. Chem.*, 4187 (2010).

[28] M.A. Bhat, S. Jain, S.K. Srivastava, R.J. Butcher, J. Wakira. *Acta Cryst.*, **E72**, 196 (2016).

[29] M.A. Bhat, S.K. Srivastava, P. Sharma, A. Chopra, R.J. Butcher, IUCrData 1, 2016, x160168, https://doi.org/10.1107/S2414314616001681

[30] M.A. Bhat, M.A. Mir, J. Agim, R.J. Butcher, S.K. Srivastava. *Inorg. Chem. Commun.*, **8**, 76 (2017).

[31] M.A. Bhat, S.H. Lone, M.A. Mir, S.A. Majid, S.K. Srivastava. *Appl. Organomet. Chem.* (2018); e4329. https://doi.org/10.1002/aoc.4329.

[32] M.A. Bhat, S.H. Lone, M.A. Mir, S.A. Majid, H.M. Bhat, R.J. Butcher, S.K. Srivastava. *J. Mol. Struct.*, **1164**, 516 (2018).

[33] M.A. Bhat, S.H. Lone, S.K. Srivastava. *Inorg. Chim. Acta* (2018) https://doi.org/10.1016/j.ica.2018.04.011

[34] W.L.F. Armarego, D.D. Perrin, "Purification of Laboratory Chemicals", 4th Edn. (1998).

[35] M.J. Frisch, G.W. Trucks, H.B. Schlegel, G.E. Scuseria, M.A. Robb, J.R. Cheeseman, G. Scalmani, V. Barone, B. Mennucci, G.A. Petersson, H. Nakatsuji, M. Caricato, X. Li, H.P. Hratchian, A.F. Izmaylov, J. Bloino, G. Zheng, J.L. Sonnenberg, M. Hada, M. Ehara, K. Toyota, R. Fukuda, J. Hasegawa, M. Ishida, T. Nakajima, Y. Honda, O. Kitao,

H. Nakai, T. Vreven, J.A. Montgomer, Jr., J.E. Peralta, F. Ogliaro, M. Bearpark, J.J. Heyd, E. Brothers, K.N. Kudin, V.N. Staroverov, T. Keith, R. Kobayashi, J. Normand, K. Raghavachari, A. Rendell, J.C. Burant, S.S. Iyengar, J. Tomasi, M. Cossi, N. Rega, J.M. Millam, M. Klene, J.E. Knox, J.B. Cross, V. Bakken, C. Adamo, J. Jaramillo, R. Gomperts, R.E. Stratmann, O. Yazyev, A.J. Austin, R. Cammi, C. Pomelli, J.W. Ochterski, R.L. Martin, K. Morokuma, V.G. Zakrzewski, G.A. Voth, P. Salvador, J.J. Dannenberg, S. Dapprich, A.D. Daniels, O. Farkas, J.B. Foresman, J.V. Ortiz, J. Cioslowski, D.J. Fox, Gaussian 09, Revision B. 01, Gaussian, Inc., Wallingford, CT (2010).

[36] (a) A.D. Becke. *J. Chem. Phys.*, **98**, 5648 (1993). (b) P.J. Stephens, F.J. Devlin, C.F. Chabalowski, M.J. Frisch. *J. Phys. Chem. B*, **98**, 1162 (1994).

[37] (a) A.D. McLean, G.S. Chandler. *J. Chem. Phys.*, **72**, 5639 (1980). (b) K. Raghavachari, J.S. Binkley, R. Seeger, J.A. Pople. *J. Chem. Phys.*, **72**, 650 (1980). (c) J.P. Blaudeau, M.P. McGrath, L.A. Curtiss, L. Radom. *J. Chem. Phys.*, **107**, 5016 (1997). (d) A.J.H. Wachters. *J. Chem. Phys.*, **52**, 1033 (1970). (e) P.J. Hay. *J. Chem. Phys.*, **66**, 4377 (1977). (f) K. Raghavachari, G.W. Trucks. *J. Chem. Phys.*, **91**, 1062 (1989). (g) R.C. Binning Jr., L.A. Curtiss. *J. Comput. Chem.*, **11**, 1206 (1990). (h) M.P. McGrath, L. Radom. *J. Chem. Phys.*, **94**, 511 (1991). (i) L.A. Curtiss, M.P. McGrath, J.P. Blaudeau, N.E. Davis, R.C. Binning Jr., L. Radom. *J. Chem. Phys.*, **103**, 6104 (1995).

[38] J.M. Andrews. *J. Antimicrob. Chemotherap.*, **48**, 5 (2001).

[39] H.Q. Sun, D.R. Yuan, X.Q. Wang, X.F. Cheng, C.R. Gong, M. Zhou, H.Y. Xu, X.C.K. Fukui, T. Yonezawa, H.J. Shingu. *J. Chem. Phys.*, **20**, 722 (1952).

[40] N. Özdemir, S. Dayan, O. Dayan, M. Dinçer, N. Kalaycıoglu. *J. Mol. Phys.*, **11**, 707 (2013).

[41] R. Parr, Functional Theory of Atoms and Molecules, Oxford University Press, New York (1989).

[42] R. Parr, L. Szentpaly, S. Liu. *J. Am. Chem. Soc.*, **121**, 1922 (1999).

[43] J.F. Janak. *Phys. Rev. B*, **18**, 7165 (1978).

[44] J.P. Perdew, R.G. Parr, M. Levy, J.L. Balduz Jr. *Phys. Rev. Lett.*, **49**, 1691 (1982).

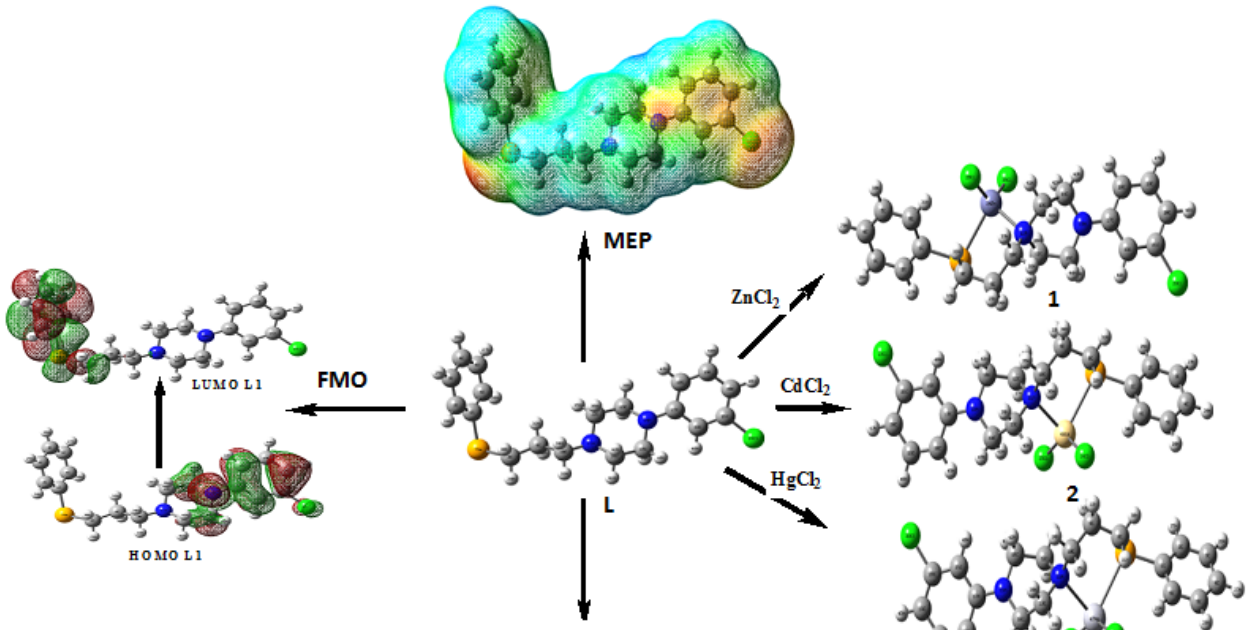

Compound	Staphylococcus aureus (MIC)	Aspergillus niger (MIC)
L^1	58	36
1	32	12
2	40	16
3	28	22
Chloromphenicol	< 1	.....
Flucanozole	...	< 1

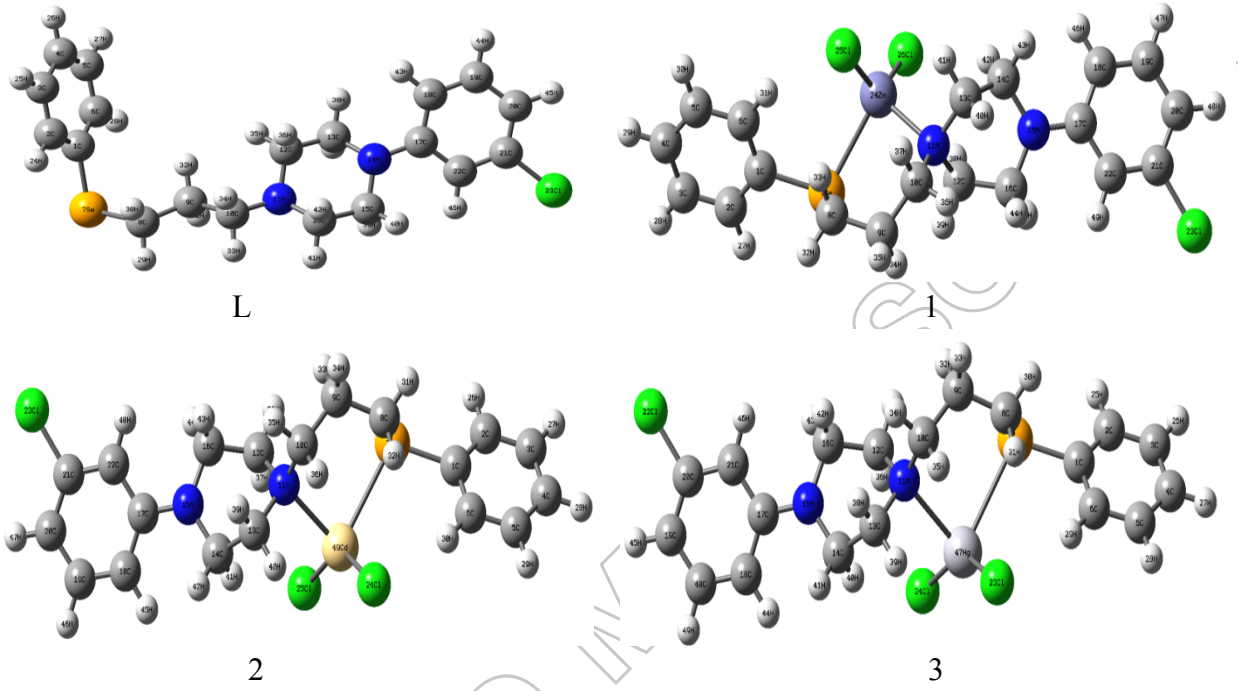

L 1

2 3

Figure 1. Optimized structures of ligand L and complexes **1-3**.

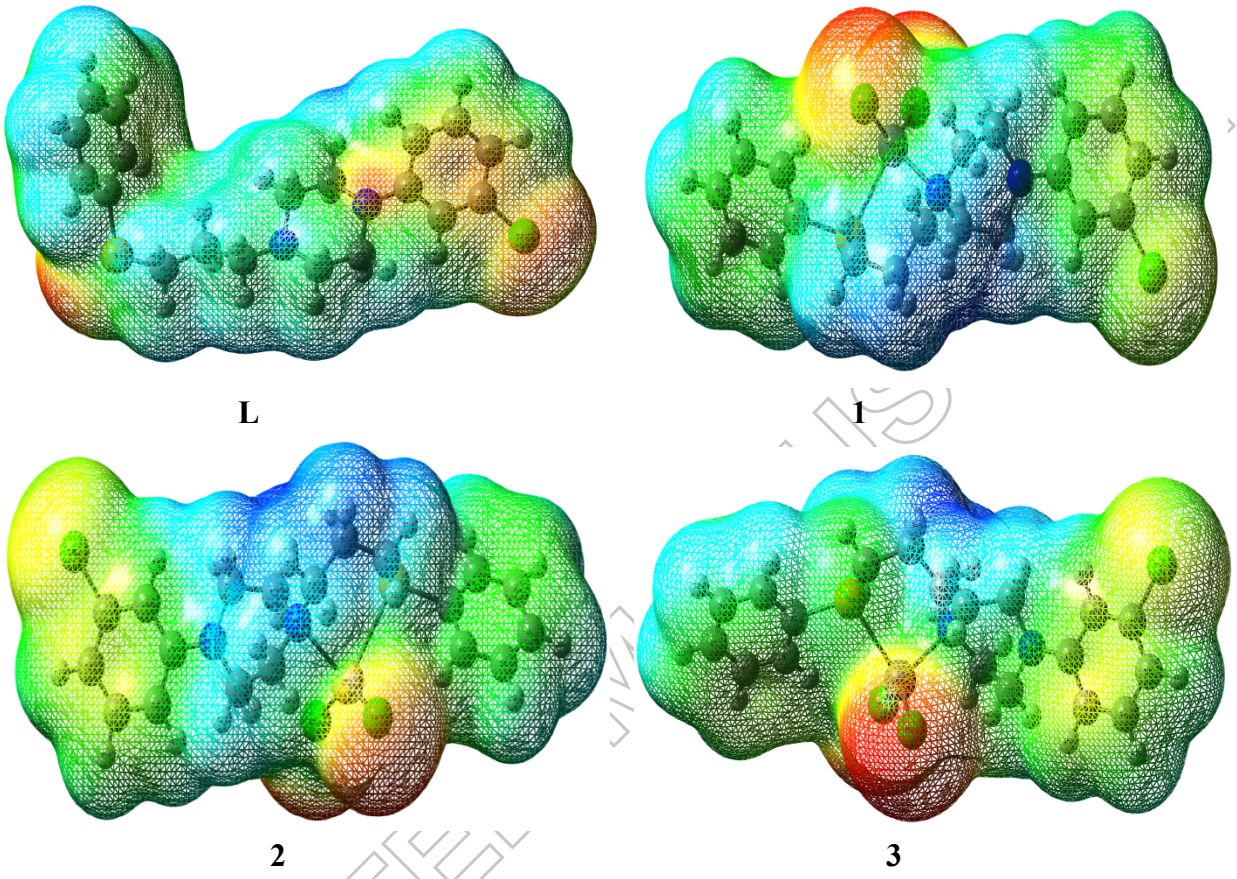

Figure 2. MEP surface of ligand L and complexes **1-3** calculated using DFT; BL3YP/LANL2DZ basis set.

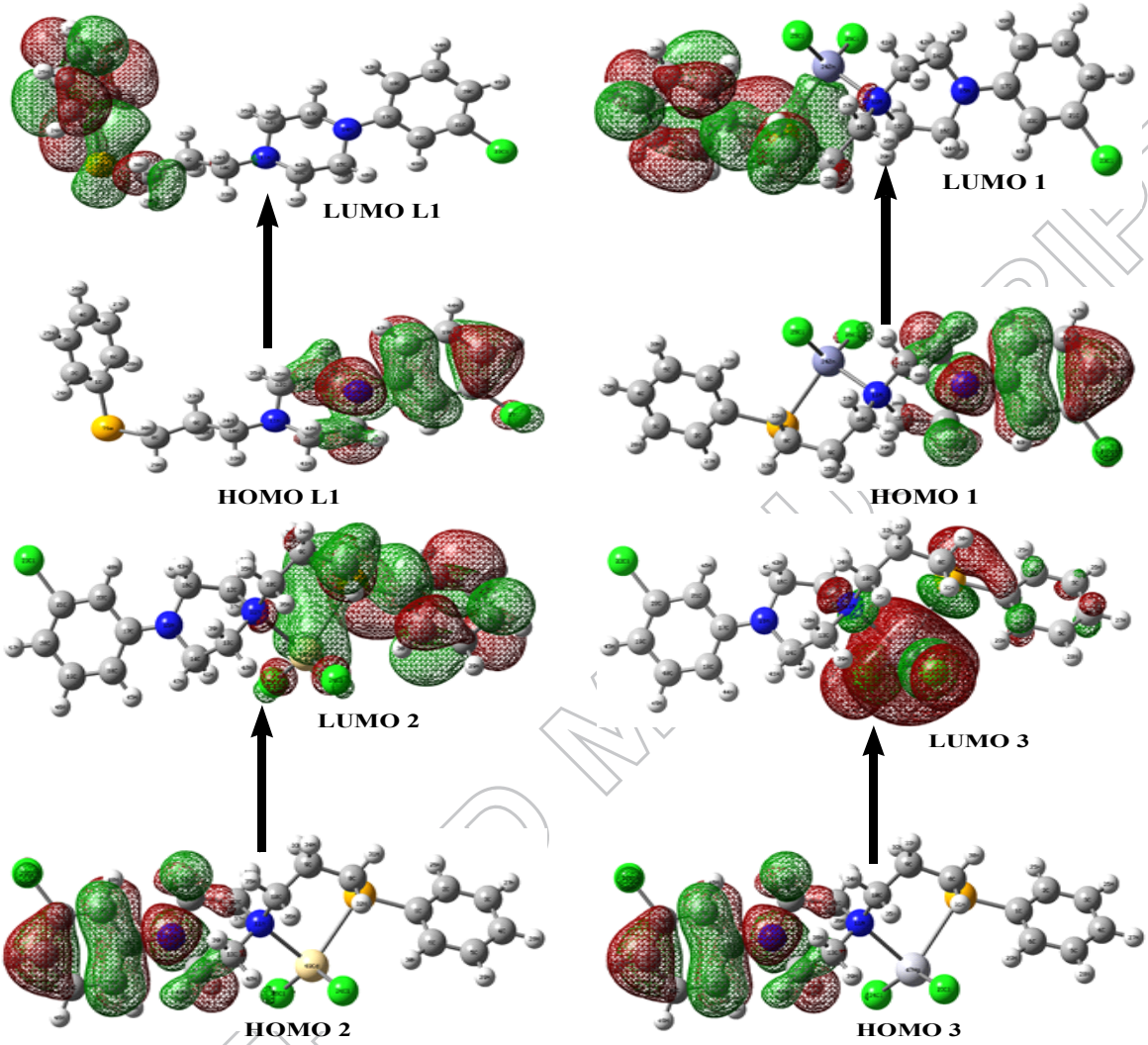

Figure 3. HOMO-LUMO surfaces of ligand L and complexes **1-3** simulated using DFT; BL3YP / LANL2DZ level of theory.

Table 1. Analytical and physical data of L and complexes **1-3**.

Ligand/ Compound	Color	Yield (%)	m.p. (°C)	Solubility	Λ_M (S cm^2 mol^{-1})
L	Cream	85	66	$CHCl_3$, MeOH, EtOH	2.95
1	White	82	123	MeOH, DMSO, DMF	3.71
2	White	78	110	MeOH, EtOH, DMSO	3.81
3	White	80	118	MeOH, EtOH, DMSO	3.45

Table 2. Selected bond lengths of ligand L and complexes **1-3** theoretically calculated at the B3LYP/LANL2DZ.

Ligand L		Complex **1**		Complex **2**		Complex **3**	
(C1-Se7)	1.92	(C1-Se7)	1.94	(C1-Se7)	1.93	(C1-Se7)	1.94
(C8-Se7)	1.97	(C8-Se7)	1.91	(C8-Se7)	1.92	(C8-Se7)	1.92
(C8-C9) 1.52		(C8-C9) 1.56		(C8-C9) 1.58		(C8-C9) 1.58	
(C9-C10)	1.53	(C9-C10)	1.59	(C9-C10)	1.60	(C9-C10)	1.60
(C10-N11)	1.46	(C10-N11)	1.51	(C10-N11)	1.51	(C10-N11)	1.51
(N11-C12)	1.46	(N11-C12)	1.40	(N11-C12)	1.46	(N11-C12)	1.46
(C12-C13)	1.52	(C12-C16)	1.46	(C12-C16)	1.52	(C12-C16)	1.52
(13C-N14)	1.46	(13C-N14)	1.58	(13C-N14)	1.54	(13C-N14)	1.54
(14C-C17)	1.40	(14C-C15)	1.40	(14C-C15)	1.48	(14C-C15)	1.48
(C17-C18)	1.41	(C17-C18)	1.35	(C17-C18)	1.35	(C17-C18)	1.35
(C20-C21)	1.38	(C20-C21)	1.54	(C20-C21)	1.53	(C20-C21)	1.35
(C21-C22)	1.39	(C21-C22)	1.35	(C21-C22)	1.35	(C21-C22)	1.35
(C21-Cl23)	1.76	(C21-Cl23)	1.76	(C21-Cl23)	1.76	(C21-Cl23)	1.76
(C22-H46)	1.08	(C22-H49)	1.07	(C22-H48)	1.07	(C22-H48)	1.07
(C12-35H)	1.09	(C12-39H)	1.07	(C12-39H)	1.06	(C12-39H)	1.06
(C9-H32)	1.09	(C9-H32)	1.07	(C9-H32)	1.07	(C9-H32)	1.07
(C1-C6) 1.39		(C1-C6) 1.54		(C1-C6) 1.53		(C1-C6) 1.53	
(C4-C5) 1.39		(Zn24-Cl25)	2.24	(Cd49-Cl25)	2.40	(Hg47-Cl24)	2.43
(C3-H25)	1.08	(Se7-Zn24)	2.36	(Se7-Cd49)	2.50	(Se7-Hg47)	2.53
(C2-H24)	1.08	(N11-Zn24)	1.94	(N11-Cd49)	2.09	(N11-Hg47)	2.11

Table 3. Selected bond angles of ligand L and complexes **1**-**3** theoretically calculated at the B3LYP/LANL2DZ.

Ligand L		Complex **1**		Complex **2**		Complex **3**	
(Se7-C1-C6)	120.20	(Se7-C1-C6)	119.99	(Se7-C1-C6)	120.00	(Se7-C1-C6)	120.00
(Se7-C8-C9)	112.58	(Se7-C8-C9)	112.90	(Se7-C8-C9)	113.91	(Se7-C8-C9)	114.19
(Se7-C8-H30)	107.32	(Se7-C8-H30)	107.50	(Se7-C8-H30)	107.11	(Se7-C8-H30)	106.99
(Se7-C1-C2)	120.07	(Se7-C1-C2)	120.00	(Se7-C1-C2)	119.98	(Se7-C1-C2)	120
(C2-1C-C6)	119.67	(C2-1C-C6)	119.99	(C2-1C-C6)	120.01	(C2-1C-C6)	120
(C8-C9-C10)	112.16	(C8-C9-C10)	114.52	(C8-C9-C10)	116.26	(C8-C9-C10)	116.52
(C9-C10-N11)	113.21	(C9-C10-N11)	119.34	(C9-C10-N11)	119.86	(C9-C10-N11)	120.03
(C10-11N-C12)	113.26	(C10-11N-C12)	113.58	(C10-11N-C12)	114.38	(C10-11N-C12)	114.41
(N11-12C-C13)	110.44	(N11-12C-C16)	126.30	(N11-12C-C16)	116.61	(N11-12C-C16)	116.60
(C12-C13-N14)	110.82	(N11-C12-C14)	111.79	(N11-C13-C14)	109.46	(N11-C13-C14)	109.48
(C13-N14-C15)	111.49	(C13-N14-N15)	111.79	(C12-C16-N15)	108.24	(C12-C16-N15)	108.25
(C13-N14-C17)	117.55	(C14-N15-C16)	107.95	(C14-N15-C16)	111.31	(C14-N15-C16)	111.30
(N14-C17-C18)	120.11	(N15-C17-C18)	119.99	(N15-C17-C18)	119.99	(N15-C17-C18)	120
(C18-C17-C22)	117.88	(C18-C17-C22)	120	(C18-C17-C22)	119.98	(C18-C17-C22)	120
(C19-C20-C21)	117.58	(Se7-Zn24-Cl25)	111.83	(Se7-Cd49-Cl25)	110.91	(Se7-Hg47-Cl24)	111.11
(C20-C21-Cl23)	119.24	(C8-Se7-Zn24)	101.29	(C8-Se7-Cd49)	101.93	(C8-Se7-Hg47)	101.79
(C19-C20-H45)	121.61	(N11-Zn24-Cl26)	110.26	(N11-Cd49-Cl25)	111.26	(N11-Hg47-Cl24)	111.66
(N11-C12-H36)	111.40	(C10-N11-Zn24)	113.56	(C10-N11-Cd49)	114.17	(C10-N11-Hg47)	114.06
(C2-C1-C6)	119.67	(C13-N11-Zn24)	119.67	(C13-N11-Cd49)	110.06	(C13-N11-Hg47)	110.07
(C6-C5-H27)	119.84	(C1-Se7-Zn24)	112.87	(C1-Se7-Cd49)	116.62	(C1-Se7-Hg47)	113.67

Table 4. Calculated energy values for ligand L and complexes **1**-**3** using B3LYP/ LANL2DZ basis set.

Parameter	L	**1**	**2**	**3**
Energy (a.u.)	-3706.995	-967.024	-949.480	-944.123
Dipole moment (Debye)	3.2244	7.9324	8.1830	7.7984
E_{HOMO} (eV)	-0.20524	-0.20819	-0.20652	-0.20599
E_{LUMO} (eV)	-0.02333	-0.05079	0.05302	-0.07397
$E_{HOMO-LUMO}$ (eV)	0.18191	0.15740	0.15350	0.13202
E_{HOMO-1} (eV)	-0.21355	-0.25409	-0.25266	-0.25167
E_{LUMO+1} (eV)	-0.01274	-0.03238	-0.03778	-0.05640
$E_{(HOMO-1)-(LUMO+1)}$ (eV)	0.20081	0.22171	0.21488	0.19527
Hardness (η)	0.09095	0.07870	0.07675	0.06601
Chemical potential (μ)	-0.11478	-0.12949	-0.12977	-0.13998
Electronegativity (χ)	0.11478	0.12949	0.12977	0.13998
Electrophilicity index (ω)	0.07237	0.10652	0.10970	0.14841

Table 5. Antibacterial and antifungal activity (MIC in μg/mL) of ligand L and complexes **1**-**3**.

Ligand/Compound	*Staphylococcus aureus*	*Aspergillus niger*
L	58	36
1	32	12
2	40	16
3	28	22
Chloromphenicol	< 1	
Flucanozole		< 1